



Visible light assisted TiO₂- chitosan composite for removal of reactive dye

A. Nithya and K. Jothivenkatachalam*

Department of Chemistry, Bharathidasan Institute of Technology, Anna University, Tiruchirappalli, TN, India

Received: 29.04.2014 Accepted: 7.09.2014

Abstract

Photocatalysis is a prominent tool for the application of environmental remediation with tremendous potential. Catalyst is immobilised onto the surface of a natural organic polymer presents a number of additional advantages including low-cost, high catalytic activity and extensive potential for reuse. The wide range of applications of natural biopolymer-chitosan for pharmaceutical, biomedical and industrial activities. In the present work, TiO₂-chitosan composite was prepared by chemical method and calcinated at 540°C. It was characterized by UV-Visible spectroscopy, UV- DRS spectroscopy, X-ray diffraction (XRD), Fourier Transformed Infrared spectroscopy (FTIR), Field Emission Scanning Electron Microscopy (FE-SEM) and Atomic Force Microscopy (AFM) techniques. Textile reactive dye Methylene Blue was used as a model pollutant to study the photocatalytic activity of the TiO₂-chitosan composite under visible light irradiation. The kinetics of photocatalytic decolourization was found to follow a pseudo-first-order according to Langmiur–Hinshelwood (L–H) model.

Keywords: Titaniumdioxide; Chitosan; Composite; Photocatalytic decolourization; Methylene Blue.

1. INTRODUCTION

Our natural environment is affected with the rapid development of science and technology. Water pollution is a major problem confronting us in the 21st century, particularly in developing countries. Many industries such as chemical, petrochemical, pharmaceutical, textile and printing industries require large quantities of water. Textile industry discharge large amount of coloured dye wastewater which is toxic, non biodegradable and threatening the whole ecosystem [1]. The decolourization of dyes effluents has always been an attractive and challenging topic. Researchers all over the world have developed extensive studies through physical-chemical, biological techniques aiming to find a cost-effective process. However, conventional physical-chemical techniques such as adsorption on activated carbon, ultra filtration, reverse osmosis, coagulation by chemical agents, and ion exchange on synthetic resins can only transfer organic compounds from one phase to another [2]. On the other hand, due to the large numbers of aromatic compounds present in dye molecules and the stability

of modern dyes, traditional biological treatment by activated sludge is ineffective for decolourization and degradation [3,4]. In recent years, heterogeneous photocatalysis was proved to be an effective advanced oxidation technique for the complete decolourization of hazardous and refractory organic compounds, due to the high oxidation potential of active hydroxyl free radical ($\bullet\text{OH}$) which is generated from irradiated semiconductor catalyst.

Heterogeneous photocatalysis using semiconductors can be more interesting than conventional methods for removing organic species in the environment. Because, the process gradually breaks down the contaminant molecule, no residue of the original material remains and therefore no sludge requiring disposal to landfill is produced. The catalyst itself is unchanged during the process and no consumable chemicals are required. This result in considerable savings and a simpler operation of the equipment involved. Additionally, the contaminant is attracted strongly to the surface of the catalyst; the process will continue to work at very low

* K. Jothivenkatachalam Tel.: +919443215423
E-mail: jothivenkat@yahoo.com



concentrations allowing sub part-per-million contents to be achieved. Taken together, these advantages mean that the process results in considerable savings in the water production cost and keeping the environment clean. The above mentioned experimental results clearly indicated that the photoexcitation of semiconductors generates electron-holes pair capable of attracting organic dyes. The strong oxidative power of photogenerated holes on semiconductor surface has made them a most suitable photocatalytic material by absorption of light for environmental remediation.

Photocatalysis using semiconductor particles has found increasing interest to solve global pollution problems, and has been proven to effectively degrade a great number of pollutants. Compared to other semiconductor photocatalysts, TiO_2 has so far been shown to be the most promising material used for both fundamental research and practical applications because it is highly photoreactive, cheap, non-toxic, chemically and biologically inert, and photostable. Although the detailed mechanism of photocatalysis varies with different pollutants, it is commonly agreed that the primary reactions responsible for the photocatalytic effect are interfacial redox reactions of electrons and holes that are generated when the semiconductor catalyst is exposed to light of sufficient energy. An only drawback is it has wide band gap energies (3.2eV) and its activity falls in UV region. Many attempts have been made to make to active in visible range via dye sensitization, metal ion doping and non-metal doping process. Transition metal doping has adverse effect on Photocatalytic activity through the formation of localized d-states in the band gap of TiO_2 . Shockley Read Hall model describes that localized d-states act as a trapping site that capture electron from conduction band or hole from valence band. Transition metal doping shortens the lifetime of mobile carriers and ultimately reduces the activity of photocatalyst. So researchers interested in non-metal doping to improve the visible light response of TiO_2 . There is an ever increasing attention for the reactivity of TiO_2 – based photocatalyst to drive reactions of environmental point of view [10].

Polymeric materials are particularly an attractive because of their controllable pore space and surface chemistry as well as their excellent mechanical strength for long-term use. The polymers are synthetic materials their biocompatibility and biodegradability are much more limited than those of natural polymers such as cellulose, chitin, chitosan and their derivatives. Chitin and chitosan are suitable functional materials because these natural polymers have excellent properties such as biocompatibility, biodegradability, non-toxicity, adsorption properties, etc. Chitosan is an

amino-polysaccharide, usually produced by partial N-deacetylation of chitin, a major component of the shells of crustacean such as crab, shrimp, and crawfish. Crab shell as well as prawn waste, mainly consists of protein (30%-40%), calcium carbonate (30%-50%) and chitin (20%-30%) on a dry basis. It is an interesting biopolymer for immobilization of desired biomolecules because of its excellent film-forming ability, high permeability, mechanical strength, nontoxicity, biocompatibility, low cost and easy availability etc. The binding ability of chitosan with metal is attributed to the chelating groups ($-\text{NH}_2$ and $-\text{OH}$ groups) present in the chitosan. The different chitosan composites such as chitosan/ TiO_2 , chitosan/cuprous oxide, chitosan/CdS and chitosan-ZnO were prepared and used to remove organics [11-16]. The aim of this present report deals with the Visible light response of TiO_2 -Chitosan biocomposite for degradation of dyes. TiO_2 -Chitosan composite was synthesized, characterised and their photocatalytic activity was evaluated on the reactive dye effluent solution under visible region.

2. EXPERIMENTAL SECTION

2.1. Materials

All the chemicals used were of analytical grade. All the solutions were prepared by using double distilled water.

2.2. Synthesis

TiO_2 -chitosan composite was prepared by 20ml of 1% chitosan in (0.1M) acetic acid and 8 ml (0.2M) sodium chloride were stirred continuously for about overnight to dissolve the chitosan flake. 1g of TiO_2 kept in contact with the viscous solution stirred continuous for about 24 hrs at 700 rpm. Then, the mixture was centrifuged and the supernatant was separated. The solid residue was filtered and washed several times with water to avoid acetic acid excess, drying under vacuum and calcined by 7 hrs at 540°C .

2.3. CHARACTERIZATION

UV-Visible spectra were recorded on Shimadzu UV-2450 spectrophotometer equipped with an integrated sphere assembly and using BaSO_4 as a reference sample. FTIR spectra were observed using a FTIR system 2000 model spectrometer by using potassium bromide pellets within $600\text{--}4000\text{cm}^{-1}$. X-ray diffraction is a versatile, non-destructive analytical method for identification and quantitative determination of various crystalline forms, known as 'phases' of compound present in powder and solid

samples. From XRD, the crystallite size can be found out by using the scherrer's formula,

$$D = \frac{K\lambda}{\beta \cos\theta} \quad (1)$$

where, D – Crystallite size, λ – Wavelength (1.54\AA), β - Full maxima half width and θ - Diffraction angle

Powder X-ray diffraction (XRD) data were collected via a Philips PW 1710 diffractometer with Cu $K\alpha$ radiation ($\lambda = 1.5418\text{\AA}$) and graphite monochromator operated at 45 kV; 30mA and 25°C. Field Emission scanning electron microscope (FE-SEM) images were taken using Carl Zeiss SIGMA instrument. Surface topography of the composite was characterized by atomic force microscopy (AFM) using Park system AFM XE 100.

2.4. Photocatalytic Activity

Photocatalytic experiments were carried out in the photo reactor “Heber visible annular type photo reactor” (Fig.1) equipped with 300 W tungsten halogen lamp (8500 lumen) was used for the investigation. The solution was illuminated with a light source at the centre of the solution reservoir, covered and separated by cylindrical quartz glass housing. Air was bubbled through the reaction solution to ensure a constant supply of oxygen and to give agitation effect to achieve equilibrium state of model pollutant and photocatalyst. For photocatalytic study, 5 mg/L concentration of MB was used. At given irradiation time interval, an aliquot amount of the samples were taken and analyzed by UV-Visible spectrometer at the wavelength of maximum absorbance for MB ($\lambda_{\text{max}} = 663 \text{ nm}$) was monitored. A calibration plot was established based on Beer-Lambert's Law by relating absorbance vs concentration.

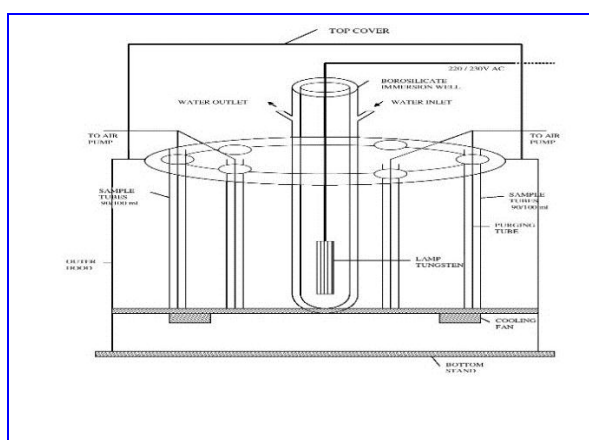


Fig. 1: Schematic diagram of the photoreactor.

The decolourisation behaviour and kinetics were studied by varying concentration of catalyst. Decolourization rate was calculated using the following equation

$$\text{Decolourization rate (\%)} = \left[\frac{C_0 - C}{C_0} \right] \times 100 \quad (2)$$

Where, C_0 is the initial concentration of dye and C is the concentration of pollutant at time t .

The reaction kinetics on photocatalyst can be expressed by the Langmuir–Hinshelwood (L–H) model.

$$\ln(C_0/C) = k_{\text{app}}t \quad (3)$$

Where, k_{app} is the apparent pseudo first order reaction rate constant and t is the reaction time. A plot of $\ln(C_0/C)$ vs t yield a slope of k_{app} .

3. RESULTS AND DISCUSSION

3.1. UV-Visible Spectra

The prepared catalyst subjected to reflectance analysis by UV-Vis DRS to find out the visible activity and band gap. The result of the spectra indicated that calcined samples show extended absorption in visible region than as prepared sample, it may be due to steep electron transition takes place between TiO_2 -chitosan composite. TiO_2 -chitosan composite has been obtained in terms of $F(R)$ values by the application of Kubelka-Munk algorithm. The band gap of the composite has been deduced from the tauc plot, the plot of $[F(R)hv]^{1/2}$ versus photon energy. The extrapolation of the rising segment of $[F(R)hv]^{1/2}$ to the abscissa at zero $F(R)$ provides the band gap energy as 3.2 eV (Fig.2) [17].

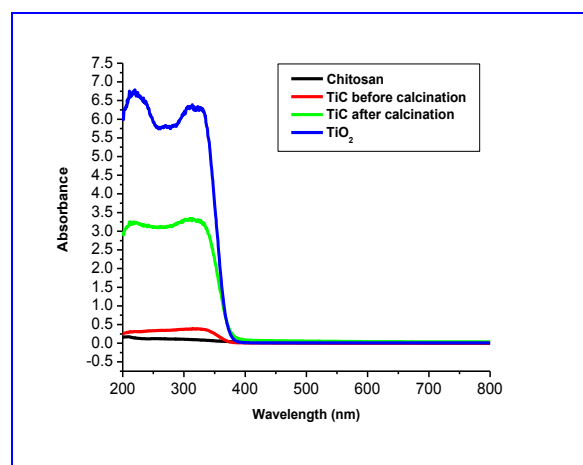


Fig. 2: UV-Visible diffuse reflectance spectra of TiO_2 -chitosan nanocomposite.

3.2 Crystallinity, Phase And Structure Analysis

The XRD pattern of TiO₂-chitosan composite shows the tetragonal structure of rutile phase. In addition to that the peak corresponds to chitosan is also observed. The average crystalline size of composite has been calculated by scherrer's equation and the size is around 34 nm and the sharp peak of XRD pattern reveals that there is no impurities present in the sample.

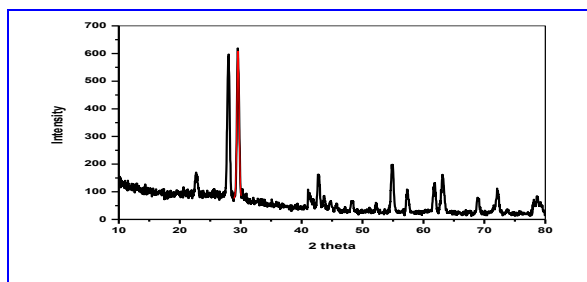


Fig. 3: XRD pattern of TiO₂-chitosan nanocomposite.

3.3. Ft-ir Spectral Study

The FT-IR spectrum of chitosan is differ from that of TiO₂-chitosan composite, peak at 3436 cm⁻¹ due to stretching vibration of hydroxyl and amino groups of chitosan. The band at 2920 cm⁻¹ was due to stretching vibration of -CH group, 1645 cm⁻¹ indicated the amide group of C-O stretching, 1421 cm⁻¹ showed the C-N axial deformation, 1388 cm⁻¹ was due to COO⁻ group of carboxylic acid. The TiO₂ - chitosan composite displayed the characteristic bands of both chitosan and TiO₂. The peak between 700-800 cm⁻¹ is an indication of Ti-O immobilization onto the chitosan.

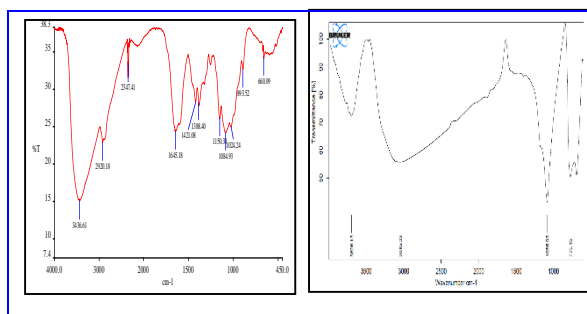


Fig. 4: FTIR spectra of (a) chitosan and TiO₂-chitosan.

3.4. Surface Area Analysis

The nitrogen adsorption-desorption isotherm of TiO₂-chitosan nanocomposite was investigated. The BET surface area of the products calculated from the BET plot is 3.907 m²/g pore radius 43 nm and the pore volume is 8.537 x 10⁻³ cc/g. The isotherm

identified as Type II is typical of macroporous material.

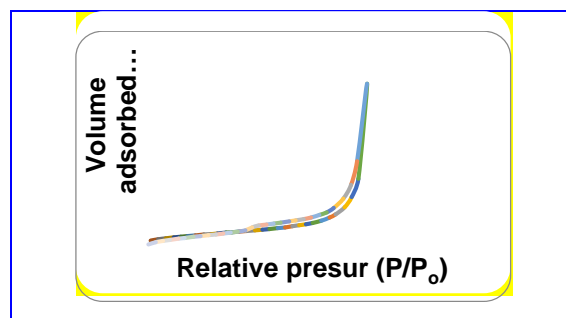


Fig. 5: Nitrogen adsorption-desorption isotherm of TiO₂-chitosan nanocomposite.

3.5. Morphological Study

Morphology is an important property in determining the effectiveness of the catalyst. FE-SEM image of the composite shows the particles size is around 120 nm. The particles are crystalline nature as shown in Fig.6.

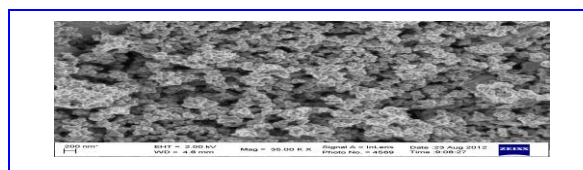


Fig. 6. FE-SEM image of nanocomposite.

Particle size has been analysed by atomic force microscopy image of nanocomposite in two dimensional and three dimensional images are shown in Fig.7. The average size of the synthesized composite around 30 nm. Particle size plays an important role in the photocatalytic activity of the catalyst. As the particle size decreases, surface area of the catalyst increases which leads to effective degradation of the dye molecules.

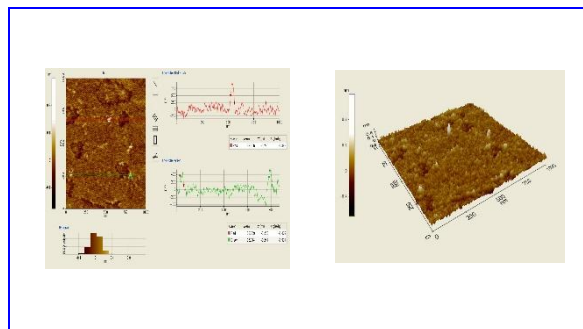


Fig. 7: AFM image of TiO₂-chitosan composite a. 2D b. 3D image

3.6. Photocatalytic Activity

The prepared catalyst is examined for photocatalytic study. Initial concentration of the dye and the catalyst amount plays an important role in the photocatalytic activity. The photocatalyst under visible light is effective as compared to dark carried out under same condition. In presence of light 100% and dark 33% is observed which proves that photodecolourization is effective as compared to adsorption process.

3.6.1. Effect Of Catalyst Amount

The photocatalyst amounts on decolorization of reactive dyes by varying from 0.1 g L^{-1} to 0.5 g L^{-1} were investigated. The dye concentration used for this study was 5 mg/L . The photocatalytic decolorization was performed for MB dye and the catalyst amount was optimised based on percentage of decolorization. Maximum of 100% was achieved for 0.3 g L^{-1} of catalyst under visible light irradiation. The effect of percentage of decolorization of MB at different amount of catalyst under visible light irradiation was presented in fig.8. The increase in the catalyst amount beyond the limit did not have an obvious positive effect on decolorization of reactive dyes because of the enhancement of light reflectance and light blocking by excessive catalyst and decrease in light penetration. Accordingly, hydroxyl radicals as the primary oxidant in photocatalytic reaction decreased and the decolorization efficiency of dye reduced [16]. The UV-Visible absorption spectra of the original dye solution and the degraded dye solution under visible light illumination after 180 min were presented in fig.9.

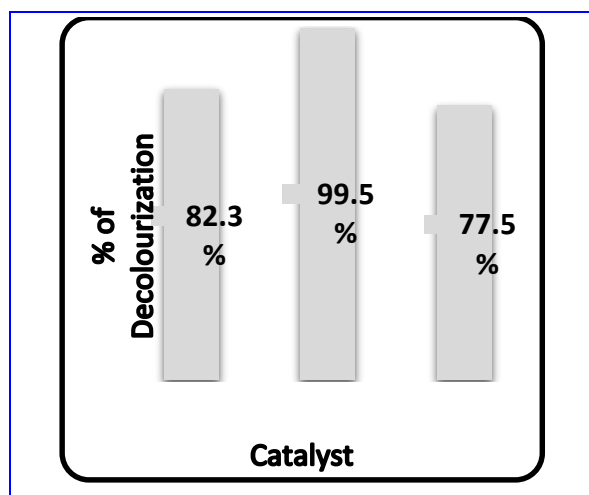


Fig. 8: The percentage of decolorization of MB at various catalyst amounts

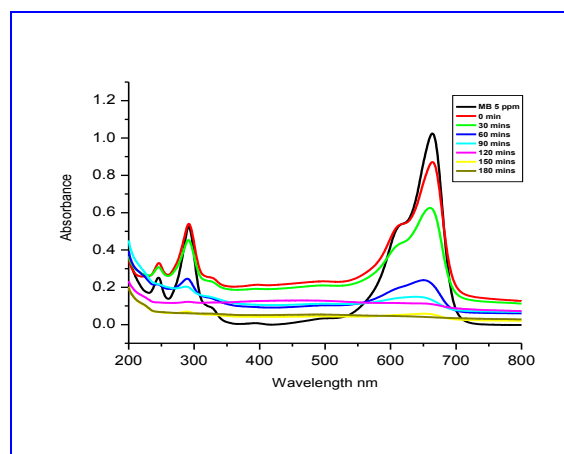


Fig. 9: The time dependent absorption spectrum for the decolorization of MB under visible light irradiation.

3.6.2. Effect Of pH

The most important parameter that influences the photocatalytic activity is dependent on pH of the solution. The efficiency of the catalyst is affected by the pH of the solution. The pH varying from 3 to 11 for the decolorization of MB at the time of 150 min. It is found that the degradation efficiency increases with increase in pH from 3 to 11. The increased efficiency in the alkaline pH may be explained on the basis of increase in the formation of $\cdot\text{OH}$ radicals with an increase in pH. The $\cdot\text{OH}$ radical is formed from the hydroxide ion of alkaline solution. A plot of $\ln(C_0/C)$ versus irradiation time of MB under visible light irradiation was presented in fig.10 and the first-order rate constant was obtained from the slop of the plots. The apparent rate constants k_{app} can be approximated as pseudo-first-order kinetics and the correlation coefficient values are highly significant as given in Table.1.

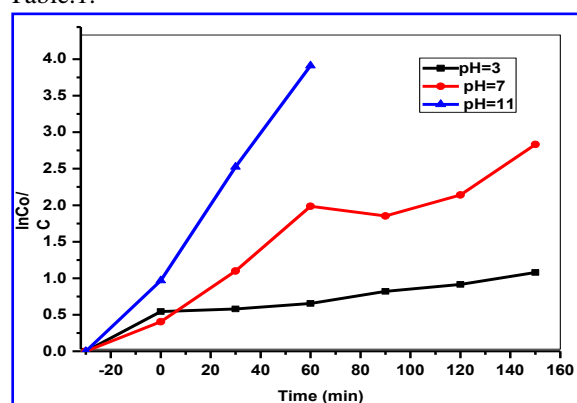


Fig. 10: Plot of $\ln(C_0/C)$ vs irradiation time under visible light irradiation for MB dye at various pH.

Table 1. Rate constant and correlation coefficient for MB under visible light irradiation at various pH

pH	Rate (min ⁻¹)	R ²
3	0.00502	0.857
7	0.01515	0.927
11	0.04431	0.987

The photocatalytic decolorization results by the rapid cleavage of chromophores, which is responsible for the colour of the dyes. Moreover, the decrease in the band gap energy adds to improve the light absorbing capacity of the catalyst and higher degree of Photocatalytic activity of the catalyst. The generation of negative carboxyl groups in the composite attracted cationic dye molecules, so that methylene blue (MB) exhibit high decolourization rate.

The decolourization of pollutants has influenced by the active site and the photo-absorption of the catalyst. The action of ionizing radiation on chitosan resulted in the polymer chain scission, accompanied by the induction of carboxyl groups in the residue. Even though irradiation induced chain scission, the chemical structure of chitosan did not change significantly. The generation of negative carboxyl groups attracted cationic dye molecules, so adsorption of basic dye is notably augmented. The repulsive interactions existed the adsorption of dye is considerable and dependent on chitosan amount and would be possible attractive interaction between π -electron cloud on the dye molecule and the cationic chitosan groups [14].

4. CONCLUSION

The TiO₂-chitosan composite was successfully prepared and characterised. The formation of composite is confirmed by UV-Visible absorption spectra and the band gap is to be 3.2 eV calculated using reflectance spectra. FT-IR analysis confirms the formation of the TiO₂-chitosan in the composite. The XRD confirms the tetragonal structure and phase purity of the sample. The morphology of TiO₂-chitosan shows the crystalline particles are in the nanometer scale. The results conclude that the TiO₂-chitosan has potential application in the decolourisation of Methylene Blue dye. The first order rate constant for the decolorization of dyes under visible light irradiation are calculated using L-H model and the correlation coefficient values are highly significant.

ACKNOWLEDGEMENT

The authors thank to Anna University – BIT Campus, Tiruchirappalli.

REFERENCES

- Kuo, W. G., Decolorizing dye wastewater with Fenton's reagent., *Water Res.*, 26, 881–886 (1992).
doi:10.1016/0043-1354(92)90192-7
- Konstantinou, I. K. and Albanis, T. A., TiO₂-assisted photocatalytic degradation of azo dyes in aqueous solution: kinetic and mechanistic investigations, *Appl. Catal. B Environ.*, 49, 1–14 (2004).
doi:10.1016/j.apcatb.2003.11.010
- An, H., Yi, Q., Gu, X. S. and Tang, W.Z., Biological treatment of dye wastewaters using an anaerobic-oxic system., *Chemosphere.*, 33, 2533–2542 (1996).
doi:10.1016/S0045-6535(96)00349-9
- Li, Y. and Xi, D. L., Decolourization and biodegradation of dye wastewaters by a facultative-aerobic process., *Environ. Sci. Pollut. Res. Int.*, 11, 372–377 (2004).
doi:10.1007/BF02979654
- Sobczynsk, A., Duczmal, L. and Dobosz, A., Photocatalysis by illuminated titania: oxidation of hydroquinone and p-benzoquinone., *Monatsh. Chem.*, 130, 377–384 (1999).
doi:10.1007/PL00010219
- Li, X., Zhao, W. and Zhao, J., 2002. Visible light-sensitized semiconductor Photocatalytic degradation of 2, 4-dichlorophenol., *Sci. China Ser. B.*, 45 (4) 421–425 (2002).
doi:10.1360/02yb9054
- Vulliet, E., Emmelin, C., Chovelon, J. M., Guillard, C. and Herrmann, J. M., Photocatalytic degradation of the herbicide cinosulfuron in aqueous TiO₂ suspension., *Environ. Chem. Lett.*, 1, 62–67 (2003).
doi:10.1007/s10311-002-0008-1
- Herrmann, J. M., Heterogeneous photocatalysis: state of the art and present applications., *Top. Catal.*, 34(4), 49–65 (2005).
doi:10.1007/s11244-005-3788-2
- Joshi, M. M., Labhsetwar, N. K., Mangrulkar, P. A., Tijare, S. N., Kamble, S. P. and Rayalu, S. S., Visible light induced photoreduction of methyl orange by N-doped mesoporous titania., *Appl Catal.*, 357, 26 (2009).
doi:10.1016/j.apcata.2008.12.030
- Zhao, J., Chen, C. and Ma, W., Photocatalytic degradation of organic pollutants under visible light irradiation., *Top. Catal.*, 35(3), 269–278 (2005).

- [doi:10.1007/s11244-005-3834-0](https://doi.org/10.1007/s11244-005-3834-0)
Zainal, Z., Hui, L. K., Hussein, M. Z. O., Abdullah, A. H. and Hamadneh, I. R., Characterization of TiO₂-chitosan/glass photocatalyst for the removal of a monoazo dye via photodegradation adsorption process., *J. Hazard. Mater.*, 164, 138–145(2009).
[doi:10.1016/j.jhazmat.2008.07.154](https://doi.org/10.1016/j.jhazmat.2008.07.154)
- Chen, J. Y., Zhou, P. J., Li, J. L. and Wang, Y., Studies on the photocatalytic performance of cuprous oxide/ Chitosan nanocomposites activated by visible light., *Carbohydr. Polym.*, 72, 128–132(2008).
[doi:10.1016/j.carbpol.2007.07.036](https://doi.org/10.1016/j.carbpol.2007.07.036)
- Zhu, H., Jiang, R., Xiao, L., Chang, Y., Guan, Y., Li, X. and Zeng, G., Photocatalytic decolorization and degradation of Congo Red on innovative crosslinked Chitosan/nano-CdS composite catalyst under visible light irradiation., *J. Hazard. Mater.*, 169, 933–940 (2009).
[doi:10.1016/j.jhazmat.2009.04.037](https://doi.org/10.1016/j.jhazmat.2009.04.037)
- Salehi, R., Arami, M., Mahmoodi, N. M., Bahrani, H. and Khorramfar, S., Novel biocompatible composite (Chitosan-zinc oxide nanoparticle): Preparation, characterization and dye adsorption properties., *Colloid Surf B.*, 80, 86–93 (2010).
[doi:10.1016/j.colsurfb.2010.05.039](https://doi.org/10.1016/j.colsurfb.2010.05.039)
- Jiang Ru., Zhu Huayue., Li Xiaodong. and Xiao Ling., Visible light photocatalytic decolourization of C. I. Acid Red 66 by chitosan capped CdS composite nanoparticles., *Chem Eng J.*, 152, 537–542 (2009).
[doi:10.1016/j.cej.2009.05.037](https://doi.org/10.1016/j.cej.2009.05.037)
- Karunakaran, C., Vijayabalan, A., Manikandan, G. and Gomathisankar, P., Visible light photocatalytic disinfection of bacteria by Cd-TiO₂., *Catal. Comm.*, 12, 826–829 (2011).
[doi:10.1016/j.catcom.2011.01.017](https://doi.org/10.1016/j.catcom.2011.01.017)